INSTITUTE OF FUNDAMENTAL TECHNOLOGICAL RESEARCH

POLISH ACADEMY OF SCIENCES

Pawińskiego 5B; 02-106 Warsaw, Poland, PHONE (+ 48) 22 8261281, FAX (+ 48) 22 8269815
http://www.ippt.pan.pl

EXPERT OPINION

addressing an inquiry posted by LIVING WATER TECHNOLOGY LTD, evaluating the possible effects of the ordering party's device for structuring of water - the "Active Tray" - on water crystallization and melting, included in the RESEARCH SERVICE CONTRACT requiring using of the scientific infrastructure, signed on 17.04.2025

Abstract

Detailed systematic studies conducted using **Differential Scanning Calorimetry revealed** existence of several **effects of the Active Tray** on crystallization and melting of chemically pure water (filtered by laboratory grade reversed osmosis system). The most important directly observed and measured effects of **the device** are:

1. An increase in ice melting temperature
2. A decrease in ice melting heat
3. A decrease in heat capacity of liquid water, and
4. A decrease in heat capacity of ice

as compared to initial water.

The most important and unexpected effect of the Active LWT Tray discovered is an increase in the Gibbs Free Energy (a thermodynamic potential) of liquid water.

Thermodynamic analysis of obtained calorimetrically data, performed using the thermodynamic data for liquid water, available in the literature - in *National Institute of Standards and Technology* – NIST database, revealed that the **Active LWT Tray** induces a change in liquid water. Comparison of the thermodynamic equilibrium phase diagrams for initial and obtained with the **Active LWT Tray** water showed that the reason of the observed thermal effects stems from slightly **higher**, than for initial water, **thermodynamic potential of liquid LWT water**. This results in much **lower thermodynamic potential** of **ice** formed by **LWT** water than for ice formed by initial water. Much lower thermodynamic potential of **ice from LWT water** implies its much higher stability.

It is noteworthy to point a **lack in the literature** of any report on such or similar effect in chemically pure water. Thus, the obtained results should be considered as a **pioneering and extraordinarily significant scientific discovery**, and **placed under special legal protection**. Taking into account high potential of a scientific discovery, this **expert opinion** shall have a more elaborated form. Due to the fact that the discovery concerns **WATER,** it should be emphasized that, despite its confidential status, it is a first scientific report on such matter, known to the author.

It should be noted that the discovered effect does **not suggest a new additional** (there are 76 known) **anomaly** of water, as it is not an autonomous and internal but definitely induced by the external (currently undefined) action of the **Active LWT Tray**.

Moreover, currently, there are **no evidences of a new crystal ice** form (the only ice thermodynamically stable in ambient conditions is the hexagonal ice *Ih*), and obtained results clearly indicate formation, after the action of the **Active LWT Tray**, of **another liquid water phase**. This new liquid water is found to possess **higher**

thermodynamic potential (higher internal energy?), which suggests stronger interactions of the water clusters. This water while crystalizing, most probably, forms the hexagonal ice Ih, but due to stronger clusters interactions, the ice is much more stable and shows even lower thermodynamic potential, which results in its higher melting temperature.

Thus, it may be expected that many of other known properties (and anomalies) of water, after action of the **Active LWT Tray** may also alter. Thus, it is reasonable and expected to continue the started research on the effects induced by devices such as the **Active LWT Tray** on the physical properties of water. It is worth to mention, that from the presented in the Opinion results of the increase in the ice melting temperature it may be expected an increase in water evaporation temperature and lower water vapor pressure. The latter should result in lower dehydration rate, which sounds crucial from the perspective of biological processes and changes in natural environment.

In agreement with the ordering party, maintaining confidentiality, the Expert proposes and agrees to:

- Continue the started research on the effects of the LWT devices and of the technology on the physical properties of water in his field of expertise
- Address the Management of the Institute the need to establish the Water Physics Laboratory
- Manage and supervise further research and cooperate with other scientific institutions willing to work on the subject in other fields of science

Moreover, the Expert agrees to take into consideration all forms of support fostering further research and project management.

I. Theoretical basis of the method

In the Expert opinion, to better understand the obtained results, which are unexpectedly extraordinary, it is at least required to discuss the fundamentals of the theory hidden behind the method. The results obtained using *Differential Scanning Calorimetry* (DSC) method rely on a measurement of the heat flow difference between a sample in a pan and an empty reference pan. Theoretical ground of the DSC method lies in the field of physics called the thermodynamics but we limit ourselves to phase transitions and equilibrium phase diagrams.

By **DSC** method is possible to detect and measure thermal effects of the phase transitions such as crystallization (liquid-> solid crystal), polymorphic transition (crystal -> crystal in solid state), crystal melting (solid -> liquid), evaporation (liquid -> vapor), which all are the phase transitions of first order. The first order phase transition produces a thermal effect, which is measured by the calorimeter. It is a latent heat effect appearing due to a change in a thermodynamic function of state, called the **enthalpy H**, which may be considered in proximity as the **internal energy** (U). The enthalpy, H, is one of the two components of the **Gibbs Free Energy, G**, a thermodynamic potential, lowering of which means higher stability of a system. This is a direct consequence of the Second Law of the Thermodynamics.

The first order phase transition leads also to a change in the second component of the Gibbs Free Energy, the **entropy, S**, which is a measure of disorder. Thus, Gibbs Free Energy, G, takes the mathematical form:

$$G(T) = H - T \cdot S$$

where T is the Absolute Temperature in Kelvin [K].

In order to easy understand the thermodynamics of the first order phase transition, scheme in the Fig. 1 illustrates a phase diagram for two phases *0* and *1*, for which the lines represent respective temperature dependences of the Gibbs Free Energy.

The temperature $\mathbf{T_{01}}$ is the equilibrium temperature of the phase transition, at which both phases *0* and *1* are in the thermodynamic equilibrium as their thermodynamic potentials are equal, $\mathbf{G_0=G_1}$. Above the $\mathbf{T_{01}}$, phase *0* is the thermodynamically stable one, but below the $\mathbf{T_{01}}$, the same is valid for phase *1*. It is determined by lower Gibbs Free Energy: $\mathbf{G_1}<G_0$ at $T<T_{01}$ and $\mathbf{G_0}<G_1$ at $T>T_{01}$. To make it more clear, in Fig. 1 , the respective lines of thermodynamic stability of each phase were plotted bold.

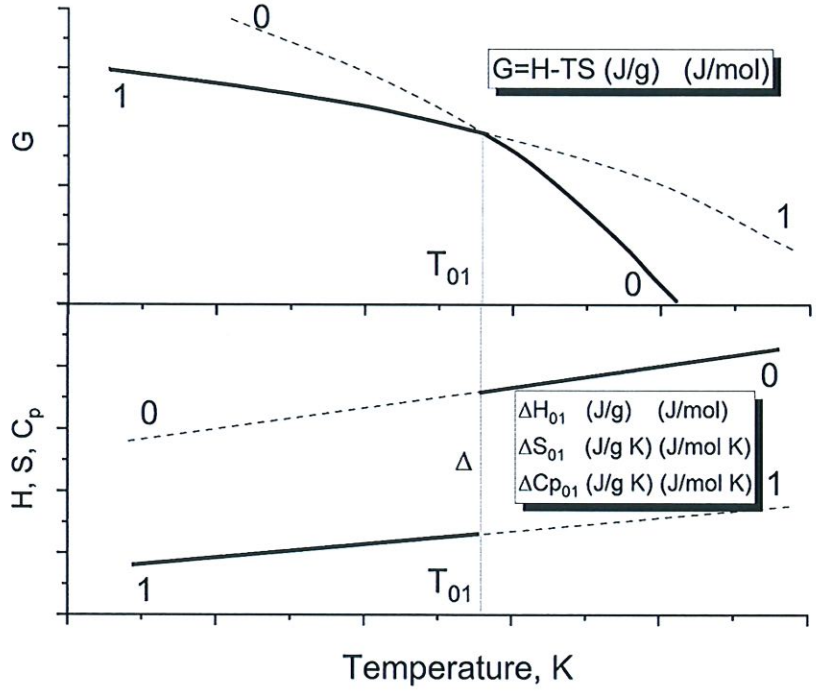

Fig. 1. Scheme of the Gibbs Free Energy (top) and the Enthalpy H, Entropy S and heat capacity Cp (bottom) changes for the first order phase transition at temperature T_{01} for two phases "0" and "1".

During the phase transition, let's say from *1* to *0*, at the temperature T_{01}, continuity of the Gibbs Free Energy is maintained; but its dependence on temperature does not. It is due to an abrupt change (delta, Δ) in the enthalpy and entropy but also in their temperature dependences: from $\mathbf{H_1}(T)$ to $\mathbf{H_0}(T)$, and from $\mathbf{S_1}(T)$ to $\mathbf{S_0}(T)$. This is shown in the bottom scheme in Fig. 1, where bold lines refer to the thermodynamically stable phases. It is clear that at T_{01}, there is a jump in enthalpy by $\mathbf{\Delta H_{01}}$, but also in entropy by $\mathbf{\Delta S_{01}}$ (change in disorder), which are bind by the transition equilibrium temperature, T_{01}:

$$\Delta S_{01} = T_{01} \cdot \Delta H_{01}$$

The enthalpy change, $\mathbf{\Delta H_{01}}$, manifesting as a thermal effect at $\mathbf{T_{01}}$ are two directly measured quantities by the DSC method. The enthalpy and entropy change but also the temperature dependences of the enthalpy and entropy manifest in the **heat capacity,** which also shows a step change at the temperature of the transition. Specific heat capacity at constant pressure, Cp, is a physical quantity and a characteristic material property defined as an amount of the heat energy required to change the temperature by 1 Kelvin taking 1 gram of a substance [J/g K].

Heat capacity, Cp, can be directly measured by the DSC method. Further, taking thermodynamic relationships between Cp and H and Cp and S, it is possible to determine the temperature dependences of the enthalpy and entropy, and thus, the Gibbs Free Energy **(G=H-T·S)**, using the integral equations:

$$H = H^0 + \int_{T^0}^{T} Cp\, dT$$

$$S = S^0 + \int_{T^0}^{T} \frac{Cp}{T}\, dT$$

where $\mathbf{H^0}$ i $\mathbf{S^0}$, are values at the temperature $\mathbf{T^0}$.

After determination of the Gibbs Free Energy, G, for the phases under consideration, it is possible to compare their thermodynamic potentials and define, for example, which one is more stable or what is (is there) a thermodynamic stability range of a particular phase.

II. The instrument and methodology

Measurements were performed using an instrumentation composed of a power compensation differential scanning calorimeter (DSC) Pyris 1 DSC and a cooling accessory Intracooler 2P produced by Perkin-Elmer (USA). The power compensation calorimeter construction is based on two separate furnaces enabling direct measurement of the heat flow difference between a sample enclosed in a pan and an empty reference pan. The instrument controls in a close loop manner the power supplied such as the both furnaces are at the same temperature. Measurement of the thermal effects or the heat capacity with the power compensation calorimeter has faster response and higher precision, especially, when compared to one-furnace calorimeters.
The Intracooler 2P provides stable cooling of the block enveloping the furnaces, down to -85 °C, what enables measurements at sub-ambient conditions at the temperature as low as -65 °C.
In the measurements there were used, provided by the producer, special hermetic stainless steel capsules sealed with a special O-ring type rubber made of Viton (Dupont). The capsules possess high chemical and corrosion resistance and sustain pressures up to 350 psi (24 atm.). The capsules enable measurements above -40 °C, due to rigidness of the rubber seal below this temperature, what may lead to lack of hermeticity. Maximum temperature should not exceed 300 °C, and in case of water samples 225 °C.
Regarding the scope of the evaluation, i.e. crystallization and melting of water, the measurements were performed in the temperature range from -40 °C and 25 °C. The cooling and heating rate applied was standard 10 K/min.

III. Results and discussion

DSC measurements revealed and confirmed existence of several effects of action of the **Active LWT Tray** on the behavior of every one of several dozen samples of chemically pure water examined, which were:

1. Changes in ice melting behavior: gradual consequent decrease and complete disappearance of the initial melting peak (melting onset at c.a. 0 °C) with simultaneous appearance, growth and perseverance of a new melting peak at higher temperature with onset at c.a. 2 °C.
2. Decrease in the ice melting enthalpy.
3. Changes in the ice crystallization behavior: gradual decrease and complete disappearance of the initial sharp crystallization peak with simultaneous appearance, in broad temperature range, of several crystallization peaks followed by a change from multi-peak crystallization to a single crystallization peak behavior.
4. Decrease in the heat capacity of the liquid water and ice.

Listed above effects are presented in the Figures 2 to 4 below for one of the samples studied, showing the changes with time in the melting and crystallization behavior after the action of the **Active LWT Tray**.

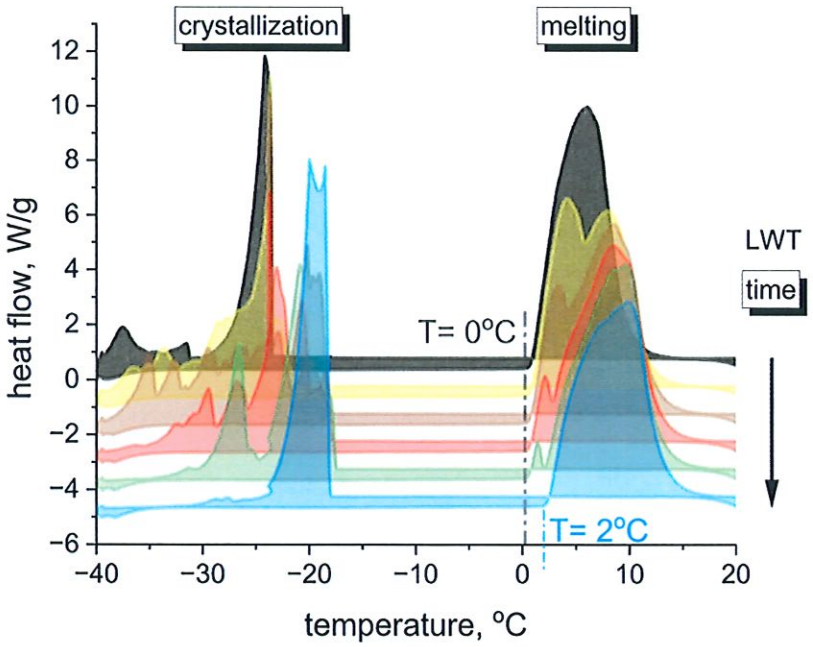

Fig. 2 Several selected measurements (cooling and heating scans) for the same sample registered at various times after the moment of action of the **Active LWT Tray.** For clarity, the curves were plotted with different color, with thermal effects of the transitions shaded, and shifted chronologically in Y axis.

On the left side of the plot in Fig. 2 (temperature lower than 0 °C), there are seen the thermal effects of crystallization. On the right side of the plot (temperature higher than 0 °C), there are seen the thermal effects of ice melting. First measurement from top (the grey curve) and the last at the bottom (the blue curve) show one thermal effect of ice melting. The most important is the difference in the onset of the ice melting, which is c.a. 2 degrees higher for the last measurement (the blue curve); for clarity, the two onsets of the ice melting are indicated by vertical dashed lines. The other measurements in the Fig. 2, registered at intermediate times, illustrate the gradual opposite changes in intensity of the two superimposed thermal effects of melting; there is clearly seen the disappearance of the melting peak starting at 0 °C with appearance and growth of the melting peak starting at 2 °C.

Fig. 2 also illustrates the changes in the crystallization behavior. First from top curve (grey one) shows mainly almost single thermal effect of ice crystallization (at c.a. -23 °C). On the following curves, in broad temperature range, there appear several superimposed crystallization effects. During the last (blue curve) measurement, there appears mainly one ice crystallization effect (at c.a. -20 °C).

In order to show in a big picture all of the changes of the thermal effects of ice melting and crystallization in the course of time from the start – action of the **Active LWT Tray** – so called "heatmap" is applied, where the heat flow is represented by a color scale from blue (lowest values) to red (highest values). This is presented in Fig. 3.

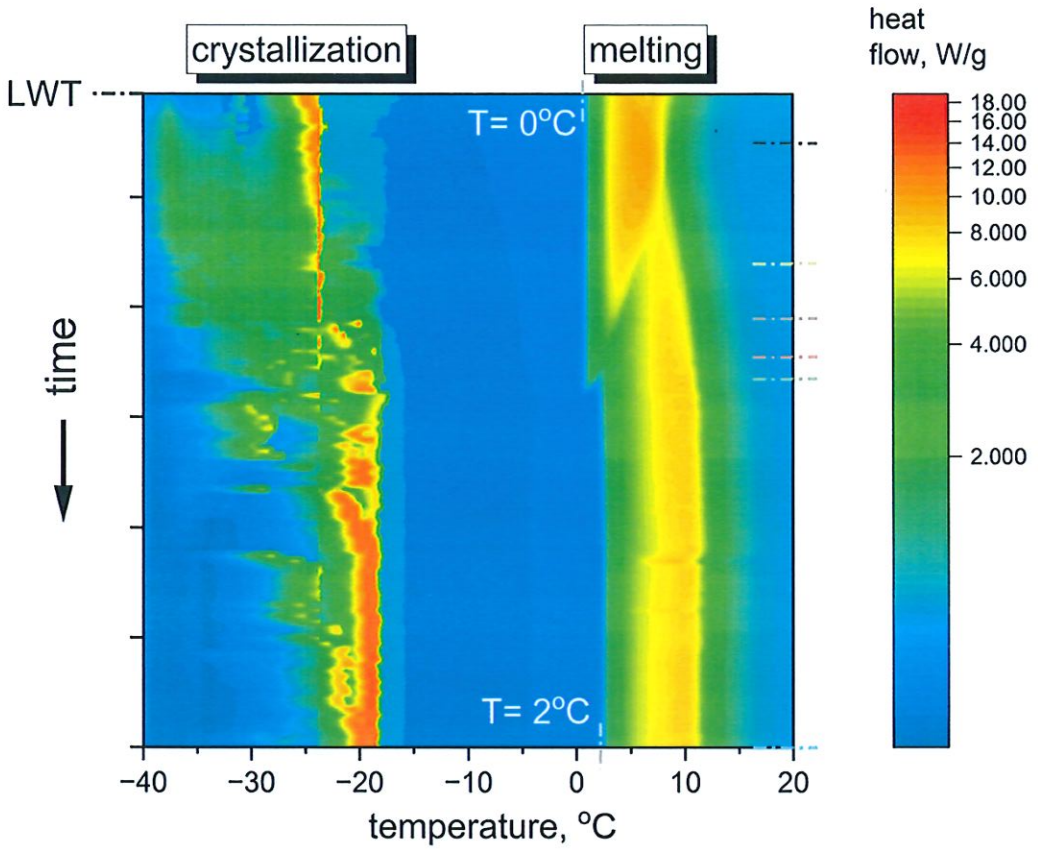

Fig. 3 Heatmap presenting changes in the thermal effects of ice melting and crystallization for a water sample as a function of time (vertical axis) from the moment of action of the **Active LWT Tray** (indicated as **LWT**) and as a function of temperature (horizontal axis). On the right edge of the heatmap, the horizontal short dashed lines in respective color correspond to the curves presented in Fig. 2. For clarity, the color scale of the heat flow (in W/g) is set logarithmic.

Further studies and deeper analysis revealed that ice crystallized from water treated with the **Active LWT Tray** not only shows melting at higher (by 2 degrees) temperature than initial water sample , but also melts with lower enthalpy change. Initially, it was concluded that this could mean a **new** crystal form of ice, different from known from the literature as hexagonal ice $I(Ih)$, which is known to be the only thermodynamically stable form at atmospheric pressure.

However, further experiments provided data indicating that the effect of the action of the **Active LWT Tray**, maybe found **in liquid water**. Precise heat capacity measurements performed on the same sample of chemically pure water, before and after treatment with the **Active LWT Tray**, revealed the effect on the heat capacity of liquid water and ice. For one of the studied samples, it was determined :

1. **Ice LWT** melting temperature 1.7 °C (274.85 K), value from the literature 0 °C (273.15 K)
2. **Ice LWT** melting enthalpy 325.84 J/g (lower by 2.4 % than value from the literature – 333.85 J/g)
3. Specific heat capacity of **liquid LWT water** 3.98 J/gK, which is lower by average by 2.6 % than measured for initial water (4.09 J/gK) and Cp of **LWT ice** lower by average by 3.2 % than measured for initial ice, for example 1.92 J/gK vs 1.98 J/gK at 273.15 K.

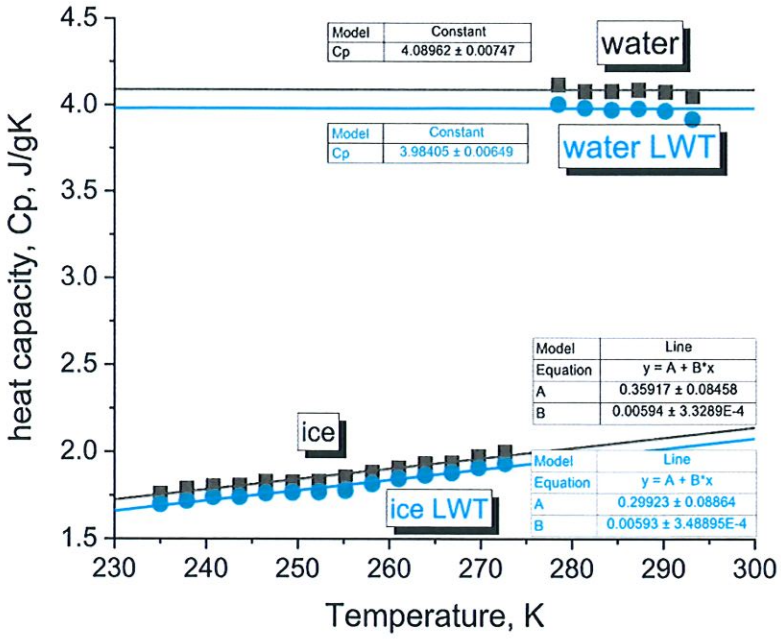

Fig. 4 Specific heat capacity, Cp, results obtained for one of the studied samples, before (shown in black) and after (shown in blue) the action of the **Active LWT Tray**, for liquid water and ice.

Further thermodynamic analysis of the data (melting temperatures, melting enthalpies, specific heat capacities of liquid water and ice) obtained for the sample before and after action of the Active LWT Tray, supported by the thermodynamic data (Cp, enthalpy H, entropy S of liquid water) available from the internet database of the *National Institute of Standards and Technology* – NIST[1], enabled determination the Gibbs Free Energy of liquid water and ice for studied sample before and after action of the Active LWT Tray. The thermodynamic phase equilibrium diagram determined is presented in Fig. 5.

[1] https://webbook.nist.gov/cgi/inchi/InChI%3D1S/H2O/h1H2

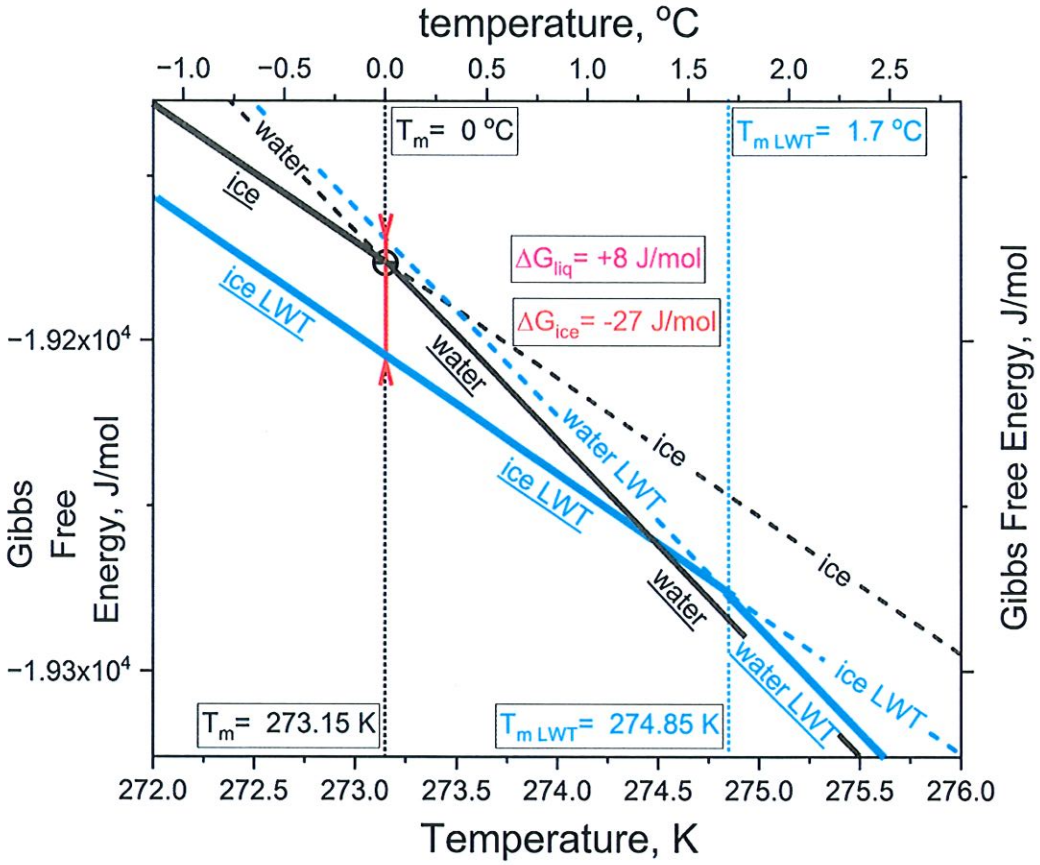

Fig. 5 Thermodynamic phase equilibrium diagram determined for one water sample before (shown in black) and after (shown in blue) action of the **Active LWT Tray**.

The diagram presented in Fig. 5 shows temperature dependences of the Gibbs Free Energy determined for liquid water and ice phases before (black) and after (blue) the action of the **Active LWT Tray**. Bold lines refer to the thermodynamic stability conditions of the phases under consideration. Dashed lines refer to conditions were the phases are thermodynamically unstable.

Both phase systems, for initial sample and after the **Active LWT Tray** action, may seem similar but shifted in temperature: for initial sample (black lines), ice phase is thermodynamically stable below 273.15 K (0 °C), and after the action of the Active LWT Tray (blue), ice phase is thermodynamically stable up to higher temperature, 274.85 K (1.7 °C). However, what is the most crucial, are the shifts in the Gibbs Free Energy levels.

The analysis results show clearly, that the **Active LWT Tray raises** the thermodynamic potential of **liquid water by (ΔG_{liq}) c.a. +8 J/mol**. This could be perceived as if the **Active LWT Tray** works against the laws of thermodynamics, however, comparison of the Gibbs Free Energy, G, of **ice** from the initial water and **ice** after the action of the **Active LWT Tray**, concurrently delivers a more pronounced **lowering** of the potential **by (ΔG_{ice}) c.a. -27 J/mol**. The meaning is that the **LWT ice** is much more thermodynamically stable than ice from initial water; and what's more, that the phase system of water obtained by action of the **Active LWT Tray** seems much more thermodynamically stable than the phase system of the initial water.

At 273.15 K (0 °C), the Gibbs Free Energies of liquid water and ice for initial water are equal, i.e. they are in thermodynamic equilibrium, what means that the driving force for the phase transition, which is ΔG= 0. For the sample treated by the **Active LWT Tray**, at this temperature, the thermodynamic driving force for transition from liquid water to ice is c.a. ΔG= -8 - 27 = -35 J/mol. With further lowering of temperature (undercooling of liquid), the driving force increases for any phase system as the difference between G of the initial and final phase, ΔG, increases. However, for the **LWT water**, the

driving force for transition is much higher than for the initial water. This may serve as preliminary justification of the just discovered, induced by the **Active LWT Tray**, process and tendency of formation of the new thermodynamically more favored phase (structure) of water.

IV. Conclusions and comments

According to the information provided by the manufacturer, the Active LWT Tray applied in the study is one of many elementary devices used for structuring water. Thus, there may be expected similar effects of action on water by the devices of same construction.

Moreover, obtained results and conclusions indicate that we possibly have just spotted (in a positive sense) the proverbial tip of the iceberg. The question is how much of the iceberg we manage to unveil and understand using nowadays technology.

Thirst for knowledge gives rise to questions like:

- Why is the observed effect so time-dependent?
- Is it possible to improve the technology by increasing the power of action and rate of the process?
- Are there conditions that the phenomenon is absent?

While searching for the answers for questions alike, it is maybe worth to consider modifications of the water structuring devices but also the techniques, instrumentation and methodology used in current research. It may be also worth to become more open for emerging or unconventional techniques, which may backwind the current technology into currently unknown directions.

INSTYTUT PODSTAWOWYCH PROBLEMÓW TECHNIKI
POLSKIEJ AKADEMII NAUK
02-106 Warszawa, ul. A. Pawińskiego 5B
NIP: 525-000-89-79

25-07-2025

dr inż. Arkadiusz Grabias

V. Scientific output of the Expert, source Web of Science

PhD Eng. Arkadiusz Gradys

Hirsh index (H-index) 18, research papers 42, citations (without self-citations) 1312

PhD thesis

2010-11-25 Polymorphic transitions in low molecular weight substances and polymers
Material Sciences, supervisor – Prof. PhD Hab. Eng. Paweł Sajkiewicz, IPPT PAN

List of the most important scientific papers (corresponding author) in chronological order from the newest:

1

On the Structural and Biological Effects of Hydroxyapatite and Gold Nano-Scale Particles in Poly(Vinylidene Fluoride) Smart Scaffolds for Bone and Neural Tissue Engineering

Zaszczynska, A; Zychowicz, M; (...); Sajkiewicz, PL Mar 2025 MOLECULES 30 (5)

Piezoelectric materials, due to their ability to generate an electric charge in response to mechanical deformation, are becoming increasingly attractive in the engineering of bone and neural tissues. This manuscript reports the effects of the addition of nanohydroxyapatite (nHA), introduction of gold nanoparticles (AuNPs) via sonochemical coating, and collector rotation speed on the formation of electroactive phases and biological properties in electrospun nanofiber scaffolds consisting of poly(vinylidene fluoride) (PVDF). FTIR, WAXS, DSC, and SEM results indicate that introduction of nHA increases the content of electroactive phases and fiber alignment. The collector rotational speed increases not only the fiber alignment but also the content of electroactive phases in PVDF and PVDF/nHA fibers. Increased fiber orientation and introduction of each of additives resulted in increased SFE and water uptake. In vitro tests conducted on MG-63 and hiPSC-NSC cells showed increased adhesion and cell proliferation. The results indicate that PVDF-based composites with nHA and AuNPs are promising candidates for the development of advanced scaffolds for bone and neural tissue engineering applications, combining electrical functionality and biological activity to support tissue regeneration.

95 References

2

Toward a Better Understanding of the Gelation Mechanism of Methylcellulose via Systematic DSC Studies

Niemczyk-Soczynska, B; Sajkiewicz, P and Gradys, A May 2022 POLYMERS 14 (9)

A methylcellulose (MC) is one of the materials representatives performing unique thermal-responsive properties. While reaching a critical temperature upon heating MC undergoes a physical sol-gel transition and consequently becomes a gel. The MC has been studied for many years and researchers agree that the MC gelation is related to the lower critical solution temperature (LCST). Nevertheless, a precise description of the MC gelation mechanism remains under discussion. In this study, we explained the MC gelation mechanism through examination of a wide range of MC concentrations via differential scanning calorimetry (DSC). The

results evidenced that MC gelation is a multistep thermoreversible process, manifested by three and two endotherms depending on MC concentration. The occurrence of the three endotherms for low MC concentrations during heating has not been reported in the literature before. We justify this phenomenon by manifestation of three various transitions. The first one manifests water-water interactions, i.e., spanning water network breakdown into small water clusters. It is clearly evidenced by additional normalization to the water content. The second effect corresponds to polymer-water interactions, i.e., breakdown of water cages surrounded methoxy groups of MC. The last one is related to the polymer-polymer interactions, i.e., fibril hydrophobic domain formation. Not only did these results clarify the MC crosslinking mechanism, but also in the future will help to assess MC relevance for various potential application fields.

15 Citations, 44 References

3

Geometrical effects during crystallization under confinement in electrospun core-shell fibers. DSC study of crystallization kinetics

Gradys, A Jan 13 2017 POLYMER 108 , pp.383-394

Calorimetric studies on poly(ethylene glycol) Mn = 400 g mol(-1), encapsulated in polystyrene fibers show non-trivial crystallization behavior. Analysis, assuming constant Avrami exponent n, is unsuitable. Approach allowing for changes in the exponent n, requires assumption of the crystallization rate function, derived from the nucleation theory. Changes in Avrami exponent n, follow the changes in geometry of crystal growth and in nucleation mechanisms. Crystallization in micrometer fibers starts from heterogeneous nucleation with three-dimensional crystal growth - as in bulk - but changes to two and one-dimensional, terminated by homogenous nucleation. For bulk and in I and 0.6 mu m thick fibers, the approach evidences similar thermodynamic parameters. In 0.6 pm thick fibers, crystallization rate is lower due to higher energy barrier for diffusion, E-D = 10 kJ mol(-1) versus 8.7 kJ mol(-1) for bulk and 1 pm thick fibers. Additionally, fiber thickness depends not only on parameters of the electrospinning process but also on the thermal history.

12 Citations, 40 References

4

Kinetics of isothermal and non-isothermal crystallization of poly(vinylidene fluoride) by fast scanning calorimetry

Gradys, A; Sajkiewicz, P; (...); Schick, C Jan 15 2016 POLYMER 82 , pp.40-48

Crystallization from melt of poly(vinylidene fluoride) was studied by thin film chip calorimetry at cooling rates from 500 to 100,000 Ks(-1) and isothermally down to 76 degrees C. At ca. 70 degrees C, for cooling rates higher than 2000 Ks(-1), there appears a change in crystallization from high temperature alpha phase to low temperature beta phase. The amorphous state is preserved at cooling rate 100,000 Ks(-1). Analysis of the crystallization kinetics with Ziabicki model reveals maximum of the steady-state crystallization rate of beta phase as 2200 s(-1) at 22 degrees C, and the highest crystallization rate of alpha phase as 200 s(-1) at 70 degrees C. Approximation of the temperature dependent steady-state crystallization rate with the Turnbull and Fisher nucleation model results in the equilibrium melting temperatures 227 and 173 degrees C for the alpha and beta phase, respectively, and in the energy barrier for short-distance transport, E-D, as 70-80 kJ mol(-1) at high supercooling.

24 Citations, 24 References

5

Determination of the melting enthalpy of β phase of poly(vinylidene fluoride)

Gradys, A and Sajkiewicz, P May 30 2013 E-POLYMERS 13 (1)

Wide Angle X-ray Scattering (WAXS), Differential Scanning Calorimetry (DSC) and Fourier Transform Infrared spectroscopy (FTIR) analyses of phase composition and of thermal properties of PVDF samples, crystallized at temperatures 27 - 155 degrees C by casting from N,N-dimethyl formamide (DMF) solution, are reported. Samples obtained at 27 degrees C contain only beta crystal phase and with increase of casting temperature content of beta phase decreases in favor of alpha phase. Evaluation of combined: phase content (WAXS) and melting heat (DSC), leads to two fold higher than for 100 % alpha phase value of 100% beta melting enthalpy, Delta H-beta(0)=219.7 J.g(-1), which may be justified by strong polar interactions in beta phase TTT conformation. The relation Delta H-beta(0)> Delta H-alpha(0) leads either to the thermodynamic stability of beta phase in whole temperature range (if T-m beta (0) >= T-m alpha (0)) or to the limited temperature range of thermodynamic stability of a phase (if T-m beta (0) < T-m alpha (0)).

16 Citations, 35 References

6

Crystallization of poly(vinylidene fluoride) during ultra-fast cooling

Gradys, A; Sajkiewicz, P; (...); Schick, C 9th Lahnwitz Seminar on Calorimetry, Sep 15 2007 THERMOCHIMICA ACTA 461 (1-2) , pp.153-157

Melt-crystallization of polyvinylidene fluoride (PVDF) was investigated in non-isothermal mode at ultra-high cooling rates ranging between 30-3000 K/s as well as at constant temperatures after quenching at 6000 K/s. An increase of the cooling rate above 150 K/s leads to the formation of P phase manifested by a low temperature shoulder of crystallization exotherm in addition to the a modification. At the cooling rates above 2000 K/s there is only low temperature exothermic peak that is attributed to the crystallization of pure beta modification. Isothermal crystallization was possible to realize at 110 degrees C as the lowest, resulting in alpha form. Much higher crystallization rate in submicrogram samples, as compared to standard DSC experiments, is also reported.

110 Citations,11 References